Macromolecules

Article

pubs.acs.org/Macromolecules

Precise Synthesis and Surface Wettability of a Polymer with Liquid Crystalline Side Chains

Tomoyasu Hirai,*[,†] Shota Osumi,[†] Hiroki Ogawa,[‡] Teruaki Hayakawa,[§] Atsushi Takahara,[∥,⊥] and Keiji Tanaka*[,†,⊥]

[†]Department of Applied Chemistry, Kyushu University, Fukuoka 819-0395, Japan

[‡]Japan Synchrotron Radiation Research Institute/SPring-8, Hyogo 679-5198, Japan

[§]Department of Organic and Polymeric Materials, Tokyo Institute of Technology, Tokyo 152-8552, Japan

[∥]Institute for Materials Chemistry and Engineering, Kyushu University, Fukuoka 819-0395, Japan

[⊥]International Institute for Carbon-Neutral Energy Research (WPI-I2CNER), Kyushu University, Fukuoka 819-0395, Japan

ABSTRACT: Well-defined poly(methacrylate)s with liquid crystal side chains, designated as PPHM, were synthesized by a living anionic polymerization method. Introducing a short-length alkyl chain at the end of the side chain, the solubility of the polymer was improved, resulting in higher molecular weight polymers. While the highest weight-average molecular weight (M_w) of PPHM was 68k, it exceeded 100k for a slight-polydisperse PPHM. Wide-angle X-ray diffraction (WAXD) revealed that PPHM formed a smectic A phase with 2.7 nm layer spacing and that the layer structure is present even in the glassy state at room temperature. Molecular aggregation states of PPHM in surface regions of films were characterized by sum-frequency generation, grazing-incidence WAXD, and contact angle measurements. The results show that the PPHM with a larger M_w formed a layer structure parallel to the film plane. Although low M_w PPHM also maintained a layer structure, the structure became more random within internal regions. The surface reorganization of PPHM with larger M_w was suppressed in comparison with smaller ones.

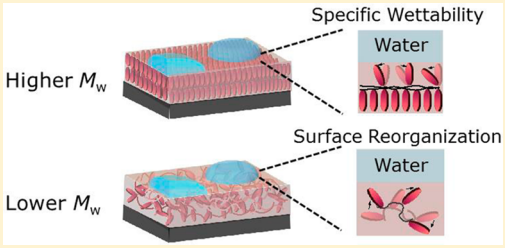

1. INTRODUCTION

The control of surface wettability is essential to create functional devices such as fuel cells,[1,2] biocompatible materials,[3,4] multilayer displays,[5] etc. Polymers with crystalline or liquid crystalline side chains have been developed to control surface wettability. The effect of molecular aggregation structures in films on surface wettability was reported for polymers consisting of alkyl side chains with carbon numbers from 1 to 17[6−8] and for fluoroalkyl chains with carbon numbers from 1 to 8.[9,10] These studies have shown that polymers with long side chains exhibit superior hydrophobicity because side chains crystallized in thin films. The side chain crystallization suppresses surface reorganization of polar groups at the polymer/water interface. The primary structure of the polymer, including the molecular weight and polydispersity index, are dominant factors governing water wettability, and other functional properties. However, relationships between surface wettability and polymer primary structures are not well established at present. Polymers that consist of crystalline or liquid crystalline side chains, and that have well-controlled molecular weights and polydispersity indexes, are needed to explicitly relate polymer primary structure to macroscopic functional properties.

Grazing-incidence X-ray diffraction (GIXD) is a superior tool to analyze nanostructures in thin films.[11−13] However, GIXD measurements cannot be used to provide structural analyses at outermost surfaces in terms of analytical depth. So far, using sum-frequency generation (SFG)[14,15] and time-dependent water contact angle[16,17] measurements, we have probed the molecular aggregation state and surface reorganization behavior at the outermost polymer/water interface for an amorphous polymer.[18−21] It is anticipated that the effect of the primary structure of the polymer on surface wettability, including the surface reorganization, may be elucidated by applying these methods to polymers with crystalline or liquid crystalline side chains, provided that the primary structure is well controlled.

Living anionic polymerization is a valuable method to precisely control the primary structure of polymers.[22,23] Using this approach, these are two main approaches to synthesize polymers with crystalline or liquid crystalline side chains. The first is to introduce side chain groups to a polymer that are prepared in advance, which is referred to as a postfunctionalization reaction.[24,25] The other is a method to polymerize a monomer with crystalline or liquid crystalline that was synthesized in advance. The former is useful for preparing polymers with narrow polydispersity indexes; however, the maximum ratio of side chain groups to polymer backbone units will be limited by steric hindrance. The latter approach is more suitable to control the molecular weight and polydispersity index when the targeted degree of polymerization is low.

Received: May 16, 2014
Revised: July 6, 2014
Published: July 18, 2014

However, due to the lack of solubility in common reaction solvents, it is difficult to achieve a high degree of polymerization.[26]

In this study, we propose to synthesize a novel monomer consisting of liquid crystalline moieties with good solubility in reaction solvents. We have examined the effect of primary structure on polymers with liquid crystalline side chains on surface wettability using polymers with precisely controlled primary structures and a high degree of polymerization that were prepared by a living anionic polymerization.

2. EXPERIMENTAL SECTION

Materials. 4′-Hydroxy-4-biphenylcarboxylic acid, methacrylic acid, and sodium were purchased from Wako Pure Chemical Industries, Ltd. Benzophenone, potassium carbonate (K_2CO_3), potassium bicarbonate ($KHCO_3$), lithium chloride (LiCl), and 1-propanol were bought from Kishida Chemical Co., Ltd. *sec*-Butyllithium (*sec*-BuLi) (1.06 M), *n*-butyllithium (*n*-BuLi) (1.08 M), 1,6-dibromohexane, 1,1-diphenyl ethylene (DPE), sodium hydroxide (NaOH), sulfuric acid (H_2SO_4), hydroquinone, acetone, *N*,*N*,-dimethylformamide (DMF), ethyl acetate, hexane, methanol (MeOH), and tetrahydrofuran (THF) were purchased from Kanto Chemical Co., Inc. Unless otherwise noted, all chemicals were used as received from the respective manufacturer. THF was freshly distilled from sodium/benzophenone under nitrogen after refluxing for at least 3 h. Prior to use, DPE was treated with a small amount of *n*-BuLi to quench the water, and was subsequently distilled.

*Synthesis of Propyl 4-(4-Hydroxyphenyl)benzoate Phenol (**1**).* 4′-Hydroxy-4-biphenylcarboxylic acid (25.0 g, 117 mmol) was dissolved in 500 mL of 1-propanol. A catalytic amount of H_2SO_4 was added to the solution. The mixture was vigorously stirred under reflux conditions. After 4 h, the excess 1-propanol was removed from the mixture using a rotary evaporator, and the resulting residue was poured into water. An NaOH solution was subsequently added to adjust the pH to 8, resulting in the formation of a precipitate. The precipitate was filtered and washed several times with distilled water. The residue was dried under vacuum and was purified by silica gel column chromatography using a mixture solvent of hexane/ethyl acetate = 1/1 as an eluent to yield (compound) **1** as a white solid (28.6 g, 96%).

^{1}H NMR (400 MHz, $CDCl_3$) δ (ppm) = 8.08−8.06 (m, −COO−*Ar*−, 2H), 7.60−7.48 (m, *Ar*, 4H), 6.93 (m, −O−*Ar*−, 2H), 5.60 (s, −O*H*, 1H), 4.29 (t, *J* = 6.59 Hz, −COO−CH_2−, 2H), 1.80 (m, *J* = 6.95 Hz, −CH_2−, 2H), 1.03 (t, *J* = 7.32 Hz, −CH_3, 3H). ^{13}C NMR (75 MHz, $CDCl_3$) δ (ppm) = 166.9, 156.0, 145.1, 132.6, 130.1, 128.6, 128.5, 126.4, 115.8, 66.6, 22.1, 10.5.

*Synthesis of 6-[4-(4-Propyl benzoate) phenoxy]hexyl Bromide (**2**).* An excess amount of 1,6-dibromohexane (135 g, 555 mmol), K_2CO_3 (25g, 178 mmol), **1** (28.5 g, 111 mmol), and 120 mL of acetone were added to a reaction flask. The reaction mixture was stirred under reflux conditions overnight. The solvent was removed from the mixture under vacuum, and the residue was purified by silica gel column chromatography with a mixture of hexane/chloroform as eluent. The ratio of chloroform in the eluent increased with increasing efflux time. Then, the compound was recrystallized from hexane to yield pure compound **2** (43.1 g, 93%).

^{1}H NMR (400 MHz, $CDCl_3$) δ (ppm) = 8.08 (d, *J* = 8.78 Hz, −COO−*Ar*−, 2H), 7.56−7.52 (m, *Ar*, 4H), 6.98−6.94 (m, −O−*Ar*−, 2H), 4.28 (t, *J* = 6.59 Hz, −COO−CH_2, 2H), 3.99 (t, *J* = 6.59 Hz, −O−CH_2−, 2H), 3.41 (t, *J* = 6.59 Hz, Br−CH_2−, 2H), 1.91−1.83 (m, −COO−CH$_2$−CH_2−, 2H), 1.80 (q, *J* = 3.66 Hz, −O−CH$_2$−CH_2−, Br−CH$_2$−CH_2−, 4H), 1.51 (q, *J* = 3.66 Hz, −CH_2−, 4H), 1.03 (t, *J* = 7.32 Hz, CH_3−, 3H). ^{13}C NMR (75 MHz, $CDCl_3$) δ (ppm) = 174.9, 166.6, 159.3, 145.1, 132.3, 130.0, 128.6, 128.3, 126.4, 114.9, 67.8, 66.5, 33.8, 32.7, 29.1, 27.9, 25.3, 22.1, 10.5.

Synthesis of 6-[4-(4-Propyl benzoate) phenoxy]hexyl Methacrylate (PHM). Methacrylic acid (14.6 g, 170 mmol) was stirred with potassium hydrogen carbonate (16.3 g, 163 mmol) for 5 min at room temperature to form the potassium methacrylate salt. The salt was added to the mixture of compound **2** (42.7 g, 102 mmol) and hydroquinone (0.30 g, 2.74 mmol) in 720 mL of DMF and the mixture was stirred overnight at 373 K. The mixture was cooled to room temperature and poured into 1.5 L of water under vigorous stirring. A precipitate was obtained as a coagulated state. The system was passed through a filter paper, and the precipitate was collected. The collected product was diluted with chloroform and dried over $MgSO_4$. Then, the system was passed once more through a filter paper, and the filtrate was evaporated. The crude product was purified by silica gel column chromatography with a mixture of hexane/chloroform = 1/1 as an eluent. Following column chromatography, the compound was recrystallized twice from hexane to yield pure PHM (27.2 g, 63%).

^{1}H NMR (400 MHz, $CDCl_3$) δ (ppm) = 7.99 (d, *J* = 8.42 Hz, −COO−*Ar*−, 2H), 7.52 (d, *J* = 8.42 Hz, *Ar*, 2H), 7.46 (d, *J* = 8.42 Hz, *Ar*, 2H), 6.88 (d, *J* = 8.42 Hz, −O−*Ar*−, 2H), 6.02 (s, CH_2═, trans, 1H), 5.46 (t, *J* = 1.46 Hz, CH_2═, cis, 1H), 4.20 (t, *J* = 6.59 Hz, −COO−CH_2−, 2H), 4.08 (t, *J* = 6.59 Hz, Ar−O−CH_2−, 2H), 3.91 (t, *J* = 6.59 Hz, −COO−CH_2−, 2H), 1.86 (s, CH_3−C−, 3H), 1.75−1.70 (m, −O−CH$_2$−CH_2−, 4H), 1.69−1.60 (m, −COO−CH_2−, 2H), 1.48−1.38 (m, −CH_2−, 4H), 0.95 (t, *J* = 7.69 Hz, CH_3−, 3H). ^{13}C NMR (75 MHz, $CDCl_3$) δ (ppm) = 167.4, 166.5, 159.2, 145.0, 136.4, 132.1, 130.0, 128.5, 128.2, 126.3, 125.2, 114.8, 67.8, 66.4, 64.5, 29.1, 28.5, 25.7, 25.7, 22.1, 18.3, 10.5. Anal. Calcd (%) for $C_{26}H_{32}O_5$: C, 73.56; H, 7.60. Found: C, 73.51; H, 7.64.

Synthesis of Poly{6-[4-(4-propyl benzoate) phenox]hexyl methacrylate} (PPHM). A 40 mL aliquot of THF was transferred to a glass reactor containing dry LiCl (32 mg, 1.3 mmol), and the glass reactor was cooled to 195 K. After 5 min, *sec*-BuLi was added to the reactor until the color changed to a slight yellow. The reactor was removed from the cooling bath to return to room temperature. This procedure made the solution colorless. The reactor was cooled back to 195 K, and *sec*-BuLi (2.5×10^{-2} mL, 2.7×10^{-2} mmol) was added. After 5 min, DPE (8.0×10^{-2} mL, 0.43 mmol) was added to the reactor and the system became deep red in color. In a Schlenk flask, PHM (1,1 g, 2.6 mmol) was dissolved in 5 mL of THF. Predissolved PHM in THF was transferred from the Schlenk flask to the reactor via a cannula under vigorous stirring. The color of the solution changed from deep red to colorless. After 4 h at 195 K, an excess amount of MeOH was added to the reactor to quench the reaction. The reaction mixture was poured into MeOH. The system was filtered, and the product was dried under a high vacuum at room temperature. PPHM (0.99 g, 90%) was obtained as a white powder.

^{1}H NMR (400 MHz, $CDCl_3$) δ (ppm) = 7.99 (br, −COO−*Ar*−, 2H), 7.50−7.43 (br, *Ar*, 4H), 6.85 (br, −O−*Ar*−, 2H), 4.23 (br, Ar−COO−CH_2−, 2H), 3.99−3.87 (br, −COO−CH_2−, Ar−O−CH_2−, 4H), 1.73 (br, main chain CH_2, 2H), 1.59−1.56 (br, −COO−CH$_2$−CH_2−, Ar−O−CH$_2$−CH_2−, 4H), 1.34 (br, Ar−COO−CH_2−, 2H), 1.02−0.98 (br, −CH_2−, 4H), 0.88 (br, CH_3−, 6H). ^{13}C NMR (75 MHz, $CDCl_3$) δ (ppm) = 166.4, 159.2, 144.8, 132.1, 130.0, 128.5, 128.2, 126.2, 114.8, 67.8, 66.4, 29.1, 28.1, 25.9, 25.8, 22.1, 10.5.

Measurements. ^{1}H and ^{13}C nuclear magnetic resonance (NMR) spectra were acquired with a JEOL JNM-ECP 400 spectrometer at 400 and 75 MHz, respectively. Gel permeation chromatography (GPC) measurements with a monodisperse polystyrene (PS) standard were carried out using a Tosoh HLC-8120 GPC with a polystyrene−divinyl benzene column (Shodex KF-804L). THF was used as an eluent with a 1.0 mL min^{-1} flow rate at 313 K. Differential scanning calorimetry (DSC) (DSC6220, SII) was carried out from 273 to 453 K at a rate of 10 K min^{-1} under a nitrogen gas flow. Polarized microscopic (POM) (Nikon ECLIPSE ME600) observations were made under a cross-Nicol condition. Film thickness was evaluated by ellipsometry (M-150, JASCO Co., Ltd.). Wide-angle X-ray diffraction (WAXD) and grazing incidence wide-angle X-ray diffraction (GIWAXD) were performed on the BL03XU beamline at SPring-8. The incidence angle of X-ray beams in the GIWAXD measurements was chosen to be 0.16°. The wettability of polymer films was evaluated by contact angle measurements using a Dropmaster DM-500, Kyowa Interface Science Co. Ltd. Water with an initial resistivity greater than 18MΩ, purified by a Milli-Q system (Millipore Co., Ltd.), was used as a probe liquid.

dx.doi.org/10.1021/ma5010265 | *Macromolecules* 2014, 47, 4901−4907

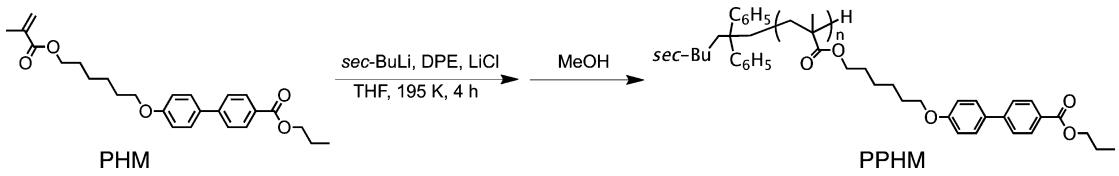

Figure 1. Synthesis of PPHM by a living anionic polymerization.

For static measurements, a water droplet with a volume of 1 μL was used. In the case of the dynamic measurements, the sample stage was tilted until a 30 μL water droplet began to slide down the substrate, and advancing (θ_a), receding (θ_r), and sliding angles (θ_s) were recorded. Local conformations of polymer chains at the outermost surfaces of films were examined using SFG spectroscopy. Films were prepared by a spin-coating method onto quartz prisms with a deposited SiO_x layer with a thickness of about 20 nm. Measurements were carried out with the *ssp* (SF output, visible input, and infrared input) polarization combination. Details of our SFG setup have been described elsewhere.[18,27]

Sample Preparation. A fiber sample of PPHM was drawn from the isotropic melt for WAXD measurements. Bulk PPHM samples for WAXD measurements were prepared by evaporating the toluene solution. Films of PPHM were prepared on silicon wafers with native oxide layers by spin-coating toluene solutions for 60 s at 3000 rpm. The film thickness, evaluated by ellipsometry was approximately 70 nm. Samples were subsequently annealed for 24 h at 358 K under a high vacuum. PPHM films in a disordered state were prepared by heating at a temperature above the isotropic phase transition temperature and successive quenching with liquid nitrogen.

3. RESULTS AND DISCUSSION

3.1. Synthesis of PPHM. In general, living anionic polymerization is an ideal synthetic method to obtain well-defined polymers. However, two difficulties lie in applying the method to a methacrylate monomer with a side chain having the methoxy biphenyl group which induces a liquid crystalline phase. The first is that there is a carbonyl group on the side chain part. As long as a conventional initiator for the living anionic polymerization, *sec*-BuLi, is used, the reaction will be unsuccessful even at a low temperature such as 195 K. This is because a highly reactive carbanion attacks carbonyl groups in monomers, resulting in side reactions that lead to the termination of the polymerization.[28] The second is that a polymer synthesized from a monomer with side chains containing the biphenyl group can be hardly dissolved in common organic solvents. This results in a limitation that a polymer with an M_w higher than ca. 20k could not be obtained.[26]

The former difficulty could be overcome by carrying out polymerization reactions under an excess amount of DPE and LiCl at low temperature.[29,30] To solve the latter problem, the monomer structure, in which the propyl ester moiety was introduced at the terminus of the biphenyl group, named PHM, was designed.

Figure 1 shows the synthesis of PPHM. To examine to what extent the degree of polymerization for PPHM impacts on the control of the polymerization, feed ratio of initiators and monomers were varied. Table 1 shows the summary of molecular weights and polydisoersity index (PDI) for PPHM obtained under various feed conditions. A liquid crystalline polymer with a M_w higher than 100k, which could be hardly obtained from a monomer with biphenyl side groups was obtained because of the improved solubility of PPHM based on the special design mentioned above. Also, it is noteworthy that

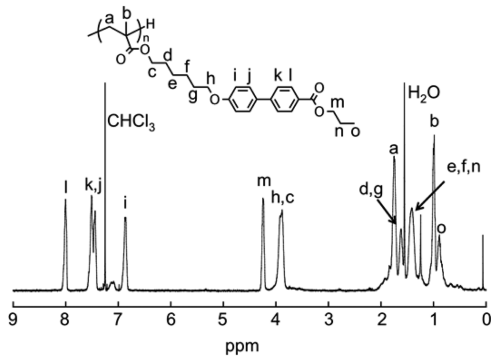

Figure 2. ^{1}H NMR spectrum of PPHM.

Table 1. M_n and PDI of PPHM

samples	M_n	M_w	M_w/M_n
poly(**1a**)	21k	22k	1.05
poly(**2a**)	46k	49k	1.06
poly(**3a**)	62k	68k	1.09
poly(**4a**)	88k	110k	1.28

PPHM has a narrow PDI. Figure 2 shows ^{1}H NMR spectrum for PPHM. All signals were clearly assigned without any contradiction. These results indicate that the living anionic polymerization of PHM can be successfully carried out under these conditions.

3.2. Aggregation States of PPHM. The formation of ordered nanostructures can be discussed on the basis of DSC, POM and WAXD measurements. Figure 3 shows DSC

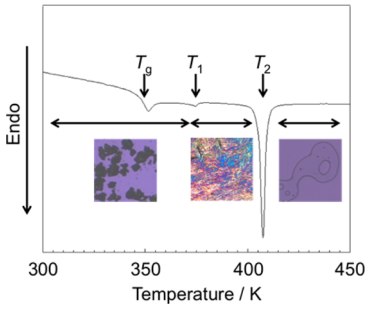

Figure 3. DSC thermograph and POM images of PPHM.

thermograms of the poly(**2a**) on the third heating scan with three POM images. The chart includes a baseline shift corresponding to T_g as well as two transition peaks, named T_1 and T_2. The fluid in the temperature range between T_1 and T_2 exhibits an optical texture. This makes it clear that the liquid crystalline phase was formed in this temperature range. The intense endothermic peak at T_2 is assigned to the phase transition from the liquid crystalline phase to the isotropic phase. The detection of the baseline shift at T_g and the smaller peak at T_1 implies that a tiny amount of chains can be

dx.doi.org/10.1021/ma5010265 | *Macromolecules* 2014, 47, 4901−4907

crystallized and the rest is vitrified on a cooling process.[26] A similar thermal behavior could be seen for other PPHM with different M_ws.

WAXD measurements were made to elucidate the detailed nanostructure of the thermodynamically stable phase. Figure 4

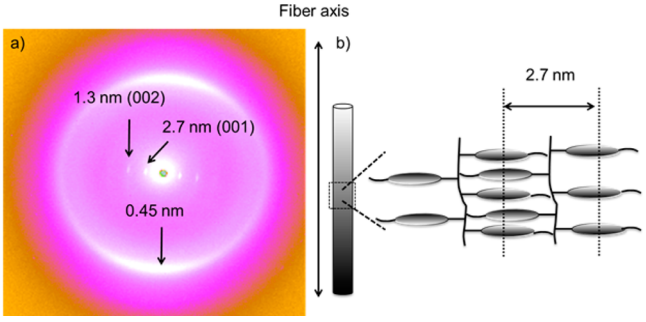

Figure 4. (a) WAXD pattern and (b) schematic illustration of aggregation structure of PPHM.

shows the WAXD pattern for a fiber form of poly(**2a**), which was drawn from the isotropic melt. The fiber axis was along the direction normal to the ground. Two reflections along the equator were observed at lower angles, namely scattering vector q values of 2.3 and 4.8 nm^{-1}. Since the larger q value is approximately twice that of the smaller one, it is apparent that there is a lamellar morphology with a domain period of 2.7 nm. Taking into account the geometry of the sample mount to the detector, it can be claimed that lamellae are formed along the direction perpendicular to the fiber axis, as shown in panel b. The distance of 2.7 nm corresponds to a calculated length between side chain portions in the fully extended form. Thus, it is conceivable that the smectic A phase with a layer thickness of 2.7 nm is formed in PPHM at a temperature range of T_1 to T_2. An intense reflection was also observed at q of 14.0 nm^{-1} along the meridian, showing that a structure with a period of 0.45 nm is formed. This value is reasonable for the distance between two adjacent biphenyl groups.[31]

PPHM aggregation states in films were examined. However, since PPHM films on silicon wafers with a native oxide layer dewetted at a temperature above T_2, the annealing was made at a temperature above the T_g by 10 K. Thick films peeled off silicon wafers that were supplied to WAXD measurements. Figure 5 shows the WAXD line profiles for nonannealed (panels a and c) and annealed (panels b and d) poly(**1a**) and poly(**2b**) films, respectively. A weak diffraction peak, corresponding to the lamellar morphology with a domain period of 2.7 nm, was observed at q = 2.3 nm^{-1} for the nonannealed poly(**1a**). On the profile for the nonannealed poly(**2a**), which is clearly different from that for poly(**1a**), one weak diffraction peak and three clear diffraction peaks are clearly seen at q = 1.4, 13.9, 15.7, and 19.0 nm^{-1}, respectively, as shown in panel c of Figure 5. Interestingly, a weak peak was observed at a smaller q than that for the nonannealed poly(**1a**).

So far, it has been reported that polymer chains with biphenyl side groups are crystallized in an orthorhombic phase.[32] Assuming that PPHM also forms the orthorhombic crystal lattice, the diffraction peaks for the nonannealed poly(**1a**) are characterized using eq 1 as follows:

$$\frac{1}{d_{hkl}^2} = \frac{h^2}{a^2} + \frac{k^2}{b^2} + \frac{l^2}{c^2} \quad (1)$$

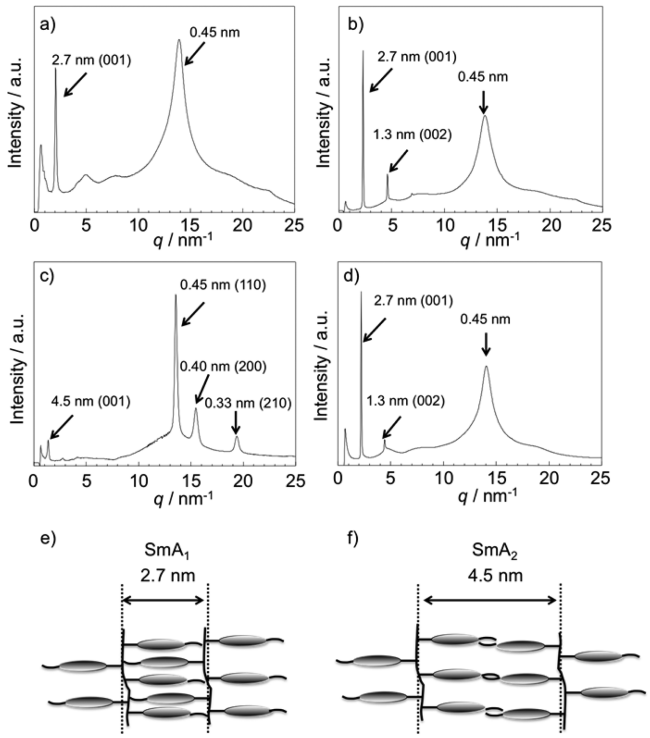

Figure 5. WAXD line profiles of nonannealed and annealed of poly(**1a**) (a and b) and of poly(**2a**) (c and d), respectively.

where h, k, l are miller plane indices, d_{hkl} is interplanar spacing, and a, b, c are lattice vectors, respectively. The a, b, and c values obtained were 0.8, 0.5, and 4.5 nm, respectively. The absence of diffraction peaks from (0kl) and (h0l) indicates that the crystal structure is not three-dimensional but two-dimensional.[26] That is, side chain biphenyl groups exist in the a−b plane and are aligned in a two-dimensional lattice with a = 0.8 nm, b = 0.5 nm, and γ = 90°. However, the layer distance of 4.5 nm is 1.7 times longer than that of the calculated side chain length, implying that nonannealed poly(**2a**) films also form during the smectic A phase but with a different periodicity, as shown in panel f of Figure 5.[33] Phases for the nonannealed poly(**1a**) and (**2a**) are defined as SmA_1 and SmA_2, respectively.

Characteristic peaks for the nonannealed poly(**2a**) corresponding to the crystallization of side chain biphenyl groups became broader after the annealing. The position of the peak at q = 1.4 nm^{-1}, namely, arisen from the SmA_2 phase, shifted after the annealing. Besides, after the annealing, the peak intensity clearly evolved and an additional peak for a higher order scattering appeared. This makes it clear that once the thermal annealing was made on the poly(**2a**) film, the aggregation states were transformed from the SmA_2 phase to the SmA_1 one. This was not the case for the poly(**1a**) film; the thermal annealing made the structural ordering of the SmA_1 phase higher, as seen in comparisons between panels a and b of Figure 5. Thus, it can be claimed that the formation of the liquid crystalline phase strongly depends on the molecular weight. In the case of PPHM, the SmA_1 phase should be thermodynamically more stable than the SmA_2 one.

GIWAXD is a powerful tool to characterize aggregation states in polymer films. Figure 6 shows GIWAXD results of nonannealed and annealed poly(**1a**) and poly(**2a**) thin films. For the nonannealed poly(**2a**), characteristic peaks were not observed for in-plane nor out-of-plane diffractions. On the

dx.doi.org/10.1021/ma5010265 | Macromolecules 2014, 47, 4901−4907

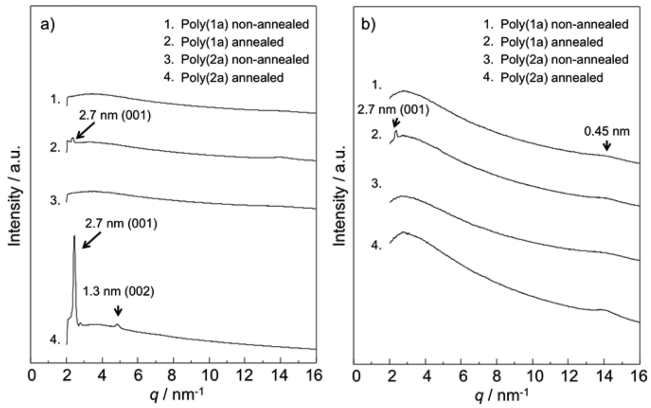

Figure 6. (a) Out-of- and (b) in-plane GIWAXD line profiles for nonannealed and annealed poly(**1a**) and poly(**2a**) films.

other hand, once the poly(**2a**) film was annealed, a clear peak corresponding to the layer distance of 2.7 nm appeared along the out-of-plane direction. A broad weak peak is also seen along the in-plane direction, which corresponds to a domain spacing of 0.45 nm. This spacing is identical to the distance between adjacent two biphenyl groups. Thus, it is conceivable that thermal annealing induces the formation of the lamellar structure in the surface region along the direction parallel to the surface.

In contrast, when the poly(**1a**) film was annealed, a weak peak corresponding to a layer distance of 2.7 nm appeared both along the in-plane and out-of-plane directions. Taking into account the sharpness of the peak, it is clear that the extent of the planar organization for the annealed poly(**1a**) film was not so striking in comparison with the poly(**2a**) film.

Poly(**1a**) is shorter than poly(**2a**). That is, the number density of ends per a volume is larger for poly(1a) than for poly(**2a**). Since the end groups possess more freedom than the repeating units, they may obscure the formation of higher order structures. Thus, the structural ordering for the annealed poly(**2a**) was better than that of poly(**1a**). End groups would be preferentially segregated at the surface due to its larger entropy.[34] If this is the case even in this study, the difference of the structural ordering between the annealed poly(**1a**) and poly(**2a**) films should be more striking in the surface region than in the internal region. This is consistent with comparison with data in Figures 5 and 6.

3.3. Surface Wettability of PPHM. The surface wettability of PPHM films before and after annealing was examined by static and dynamic contact angle measurements. Table 2 summarizes the results using water as a probe liquid. As general trends, the static contact angle for poly(**1a**) was larger than that

Table 2. Static and Dynamic Contact Angles on PPHM Films

		dynamic θ/deg			
samples	static θ/deg	θ_a	θ_r	$\Delta\theta$	θ_s
nonannealed poly(**1a**)	90.1 ± 0.3	89 ± 0.6	74 ± 0.5	15	15 ± 1.0
annealed poly(**1a**)	92.3 ± 0.3	95 ± 0.3	81 ± 1.8	14	16 ± 0.7
nonannealed poly(**2a**)	85.1 ± 0.3	89 ± 0.8	78 ± 0.8	11	17 ± 1.4
annealed poly(**2a**)	82.2 ± 0.2	86 ± 0.1	78 ± 1.3	8	7 ± 0.6

of poly(**2a**) and there are no significant differences between nonannealed and annealed samples. Taking into account M_w of poly(**1a**) and poly(**2a**), a possible explanation for the contact angle difference between the two should be related to the extent of the surface ordering. As discussed after GIWAXD results, the extent of the surface ordering was worse for poly(**1a**) than poly(**2a**), meaning that the surface entropy should be larger for poly(**1a**). If this is the case, the surface free energy becomes lower. That is, the contact angle on the surface becomes larger. Also, the annealed poly(**2a**) film exhibited the smallest sliding angle and the lowest contact angle hysteresis, $\Delta\theta_s$ ($=\theta_a - \theta_r$), in the dynamic contact angle measurement. The $\Delta\theta_s$ mainly reflects the surface roughness and reorganization.[35] The root-mean-square surface roughness for the poly(**1a**) and poly(**2a**) films was less than 1.0 nm in a 5 × 5 μm^2 scanning area. Thus, the magnitude of $\Delta\theta_s$ here corresponds to the extent of the surface reorganization, meaning that the surface of the annealed poly(**2a**) was most stable to water among the samples.

Figure 7 shows the time dependence of the static contact angle, $\theta(t)$, for the nonannealed and annealed poly(**1a**) and

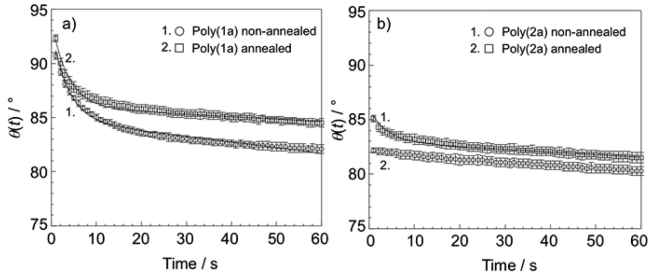

Figure 7. Time dependence of static water contact angle against (a) poly(**1a**) and (b) poly(**2a**) films, respectively.

poly(**2b**) films. Solid lines were fit to the experimental data using eq 2,

$$\theta(t) = (\theta_{ini} - \theta_{ter}) \exp\left(-\frac{t}{\tau}\right) - kt + \theta_{ter} \quad (2)$$

where θ_{ini} and θ_{ter} are the initial and terminal values of θ at $t = 0$ and in the quasi-equilibrium state, respectively, τ is the time constant for the θ decay in the initial stage, and k is a constant corresponding to the θ decrement due to water evaporation.[19] The annealing process had a large impact on the wetting behavior. In the case of the nonannealed film, the $\theta(t)$ exponentially decreased with increasing time at the initial stage, and then $\theta(t)$ monotonically decreased. On the other hand, the initial exponential decay became less dominant for the annealed film. The τ values for the nonannealed and annealed poly(**1a**) films were 3.62 and 3.68 s, respectively. On the other hand, the τ value for the nonannealed poly(**2a**) film was 3.86 s and the exponential decay was not observed after annealing. The exponential decay and monotonic decrease of $\theta(t)$ can be attributed to the surface reorganization, which can be attained by a change of local conformation, and the evaporation of water, respectively.[19] Hence, it seems that the surface reorganization of the poly(**2a**) film was suppressed after annealing. In the case of poly(**1a**) film after annealing, although the θ value increased, the initial exponential decay could be still observed. This indicates that the surface of the poly(**1a**) film was reorganized in contact with water even after annealing. On the basis of the GIWAXD results, the well-defined layer

dx.doi.org/10.1021/ma5010265 | Macromolecules 2014, 47, 4901−4907

structure parallel to the surface was formed only for the poly(**2a**) film after annealing. Thus, it seems likely that the layer structure prevents the reorganization of the surface.

To confirm the plausibility of this hypothesis, the wettability of a poly(**2a**) film quenched from the isotropic phase using liquid nitrogen was examined. Figure 8 shows the result from

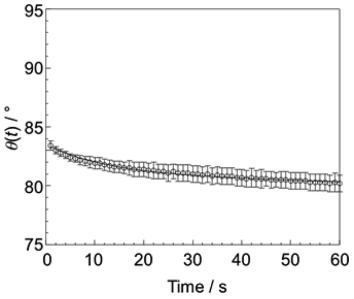

Figure 8. Time dependence of static water contact angle on a quenched poly(**2a**) film.

this experiment. The θ–t relation is quite similar to the nonannealed poly(**2a**) film, which makes it clear that the hypothesis proposed above is quite reasonable.

SFG, which currently provides the best depth resolution among available techniques, can directly detect the local conformation of chains at air and water interfaces. Panel a of Figure 9 shows the spectra for the nonannealed and annealed

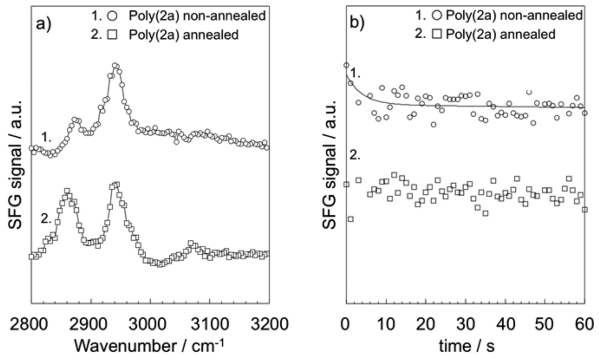

Figure 9. SFG data for nonannealed and annealed of poly(**1a**) and poly(**2a**): (a) spectra for polymer-air interface; (b) time dependence of SFG signal intensity for C–H stretching vibration of methylene groups beside the oxygen atom at polymer–water interface.

poly(**2a**) at the air/polymer interface with the *ssp* polarization combination. Appearance of an SFG peak with this polarization combination means that functional groups orient at the interface along the out-of-plane direction. The peaks around 2875 and 2960 cm^{-1} are assigned to the symmetric and antisymmetric C–H vibrations of methyl groups in side chains, respectively.[36] The former clearly evolved after annealing. Also, a characteristic peak originating from phenyl groups appeared in the wavenumber range of 3000 to 3100 cm^{-1} after annealing. These indicate that side chains aligned along the perpendicular direction after annealing and are in good accordance with the other experiments mentioned above.

Then, to what extent is the rate of the surface reorganization examined. Figure 9 (b) shows the SFG intensity at 2915 cm^{-1} corresponding to the antisymmetric C–H stretching vibration of methylene groups as a function of time. The time of 0 is defined as when water is guided onto the sample. In the case of the sample before annealing, the intensity exponentially decayed at first and then plateaued. A solid curve denotes the expectation using a single exponential function with the time constant, which was obtained by contact angle measurements shown in Figure 7b. It is noteworthy that the curve could reproduce the experimental data. On the other hand, the SFG intensity remained unchanged once the sample was annealed. This was also in good accordance with the time dependence of the contact angle. In the case of poly(**1a**), the side chain ordering at the surface was also observed after annealing. However, the surface ordering was reorganized in the presence of water. Thus, it can be concluded that the surface reorganization is controlled by the perfection of the layer structure formed in the thin film, which depends on M_w.

4. CONCLUSION

To synthesize well-defined and higher molecular weight polymers with liquid crystalline side chains, a monomer, 6-[4-(4-propyl benzoate) phenoxy] hexyl methacrylate (PHM), was designed. Since PHM possess a shorter alkyl chain at the terminus of the biphenyl group, monodisperse PPHM with a higher M_w such as 68k was successfully obtained by living anionic polymerization. Also, when the polydispersity index of 1.28 was permissible, PPHM with a M_w of 110k was obtained. To the best of our knowledge, these polymers are extremely long in length as a side-chain liquid crystalline polymer. PPHM forms a smectic A phase in the range between two transition temperatures named T_1 and T_2, which are assigned to the melting temperature and the liquid crystalline-isotropic phase transition temperature, respectively. The liquid crystalline phase is vitrified at blow T_1. The liquid crystalline structure for as-prepared films was dependent on M_w. The equilibrium structure after the thermal annealing was made at a temperature above the T_g by 10 K was the smectic A, in which lamellae aligned along the direction parallel to the surface with a periodicity of 2.7 nm. Although this structure was common for lower and higher M_w samples, the structure ordering depended on M_w. PPHM films with different M_w also exhibited variable wettability. While in the case of a lower M_w, the water sliding angle on the film remained unchanged after annealing, and became lower for the PPHM film with a higher M_w. This wetting behavior of PPHM evolves with the surface ordering of the liquid crystalline structure, depending on M_w.

AUTHOR INFORMATION

Corresponding Authors

*(T.H.) Telephone: +81-92-802-2878. Fax: +81-92-802-2880. E-mail: t-hirai@cstf.kyushu-u.ac.jp.

*(K.T.) E-mail: k-tanaka@cstf.kyushu-u.ac.jp.

Notes

The authors declare no competing financial interest.

ACKNOWLEDGMENTS

We would like to express our gratitude to Dr. Hiroyasu Masunaga in Japan Synchrotron Radiation Research Institute/SPring-8 and Dr. Misao Horigome, Mr. Masahiko Asada, and Mr. Junichiro Koike in DIC Corporation for fruitful discussions, especially concerning WAXD analysis. This research was partly supported by the Scientific Research on Innovative Areas "New Polymeric Materials Based on Element-Blocks" (No. 25102535) programs and by a Grant-in-Aid for Scientific Research (B) (No. 24350061) and by Photon and

Quantum Basic Research Coordinated Development Program from the Ministry of Education, Culture, Sports, Science, and Technology, Japan. The WAXD measurements were carried out at BL03XU at SPring-8 with the proposal number 2011B 7279, 2011B 7280, and 2012A 7228. We also thank the support from the JST SENTANKEISOKU (13A0004).

REFERENCES

(1) Costamagna, P.; Srinivasan, S. *J. Power Sources* **2001**, *102*, 242−252.
(2) Hickner, M. A.; Ghassemi, H.; Kim, Y. S.; Einsla, B. R.; McGrath, J. E. *Chem. Rev.* **2004**, *104*, 4587−4611.
(3) Yasuda, H.; Bumgarner, M. O.; Marsh, H. C.; Yamanashi, B. S.; Devito, D. P.; Wolbarsht, M. L.; Reed, J. W.; Bessler, M.; Landers, M. B.; Hercules, D. M.; Carver, J. *J. Biomed. Mater. Res.* **1975**, *9*, 629−643.
(4) Alves, N. M.; Pashkuleva, I.; Reis, R. L.; Mano, J. F. *Small* **2010**, *6*, 2208−2220.
(5) Greenham, N. C.; Moratti, S. C.; Bradley, D. D. C.; Friend, R. H.; Holmes, A. B. *Nature* **1993**, *365*, 628−630.
(6) Kim, B. G.; Sohn, E. H.; Lee, J. C. *Macromol. Chem. Phys.* **2007**, *208*, 1011−1019.
(7) Sohn, E. H.; Ahn, J.; Kim, B. G.; Lee, J. C. *Langmuir* **2011**, *27*, 1811−1820.
(8) Sohn, E. H.; Kim, S. H.; Lee, M.; Lee, J. C.; Song, K. *J. Colloid Interface Sci.* **2011**, *360*, 623−632.
(9) Katano, Y.; Tomono, H.; Nakajima, T. *Macromolecules* **1994**, *27*, 2342−2344.
(10) Honda, K.; Morita, M.; Otsuka, H.; Takahara, A. *Macromolecules* **2005**, *38*, 5699−5705.
(11) Rauscher, M.; Salditt, T.; Spohn, H. *Phys. Rev. B* **1995**, *52*, 16855−16863.
(12) Hirai, T.; Leolukman, M.; Jin, S.; Goseki, R.; Ishida, Y.; Kakimoto, M. A.; Hayakawa, T.; Ree, M.; Gopalan, P. *Macromolecules* **2009**, *42*, 8835−8843.
(13) Ogawa, H.; Masunaga, H.; Sasaki, S.; Goto, S.; Tanaka, T.; Seike, T.; Takahashi, S.; Takeshita, K.; Nariyama, N.; Ohashi, H.; Ohata, T.; Furukawa, Y.; Matsushita, T.; Ishizawa, Y.; Yagi, N.; Takata, M.; Kitamura, H.; Takahara, A.; Sakurai, K.; Tashiro, K.; Kanaya, T.; Amemiya, Y.; Horie, K.; Takenaka, M.; Jinnai, H.; Okuda, H.; Akiba, I.; Takahashi, I.; Yamamoto, K.; Hikosaka, M.; Sakurai, S.; Shinohara, Y.; Sugihara, Y.; Okada, A. *Polym. J.* **2013**, *45*, 109−116.
(14) Shen, Y. R. *Nature* **1989**, *337*, 519−525.
(15) Chen, Z.; Shen, Y. R.; Somorjai, G. A. *Annu. Rev. Phys. Chem.* **2002**, *53*, 437−465.
(16) Crowe, J. A.; Genzer, J. *J. Am. Chem. Soc.* **2005**, *127*, 17610−17611.
(17) Crowe-Willoughby, J. A.; Stevens, D. R.; Genzer, J.; Clarke, L. I. *Macromolecules* **2010**, *43*, 5043−5051.
(18) Tateishi, Y.; Kai, N.; Noguchi, H.; Uosaki, K.; Nagamura, T.; Tanaka, K. *Polym. Chem.* **2010**, *1*, 303−311.
(19) Horinouchi, A.; Atarashi, H.; Fujii, Y.; Tanaka, K. *Macromolecules* **2012**, *45*, 4638−4642.
(20) Horinouchi, A.; Tanaka, K. *RSC Adv.* **2013**, *3*, 9446−9452.
(21) Oda, Y.; Horinouchi, A.; Kawaguchi, D.; Matsuno, H.; Kanaoka, S.; Aoshima, S.; Tanaka, K. *Langmuir* **2014**, *30*, 1215−1219.
(22) Szwarc, M.; Levy, M.; Milkovich, R. *J. Am. Chem. Soc.* **1956**, *78*, 2656−2657.
(23) Szwarc, M. *Nature* **1956**, *178*, 1168−1169.
(24) Mao, G. P.; Wang, J. G.; Clingman, S. R.; Ober, C. K.; Chen, J. T.; Thomas, E. L. *Macromolecules* **1997**, *30*, 2556−2567.
(25) Hayakawa, T.; Seino, M.; Goseki, R.; Hirai, T.; Kikuchi, R.; Kakimoto, M. A.; Tokita, M.; Yokoyama, H.; Horiuchi, S. *Polym. J.* **2006**, *38*, 567−576.
(26) Yamada, M.; Iguchi, T.; Hirao, A.; Nakahama, S.; Watanabe, J. *Macromolecules* **1995**, *28*, 50−58.
(27) Tsuruta, H.; Fujii, Y.; Kai, N.; Kataoka, H.; Ishizone, T.; Doi, M.; Morita, H.; Tanaka, K. *Macromolecules* **2012**, *45*, 4643−4649.
(28) Lochmann, L.; Doskocilova, D.; Trekoval, J. *Collect Czech. Chem. C* **1977**, *42*, 1355−1360.
(29) Varshney, S. K.; Hautekeer, J. P.; Fayt, R.; Jerome, R.; Teyssie, P. *Macromolecules* **1990**, *23*, 2618−2622.
(30) Hirai, T.; Leolukman, M.; Hayakawa, T.; Kakimoto, M.; Gopalan, P. *Macromolecules* **2008**, *41*, 4558−4560.
(31) Watanabe, J.; Tominaga, T. *Macromolecules* **1993**, *26*, 4032−4036.
(32) Hahn, B.; Wendorff, J. H.; Portugall, M.; Ringsdorf, H. *Colloid Polym. Sci.* **1981**, *259*, 875−884.
(33) Ahn, S. K.; Deshmukh, P.; Gopinadhan, M.; Osuji, C. O.; Kasi, R. M. *ACS Nano* **2011**, *5*, 3085−3095.
(34) Satomi, N.; Tanaka, K.; Takahara, A.; Kajiyama, T.; Ishizone, T.; Nakahama, S. *Macromolecules* **2001**, *34*, 8761−8767.
(35) Andrade, J. D. *Surface and Interfacial Aspects of Biomedical Polymers*. Plenum Press: New York, 1985; pp 249−292.
(36) Wang, J.; Paszti, Z.; Even, M. A.; Chen, Z. *J. Am. Chem. Soc.* **2002**, *124*, 7016−7023.